Substrate-Independent and Re-Writable Surface Patterning by Combining Polydopamine Coatings, Silanization, and Thiol-Ene Reaction

Shuai Li, Johannes M. Scheiger, Zhenwu Wang, Zheqin Dong, Alexander Welle, Vanessa Trouillet, and Pavel A. Levkin*

Polydopamine coating is a unique, simple, and substrate-independent surface functionalization strategy. Techniques for secondary functionalization, patterning, and re-functionalization of polydopamine modified materials are important to broaden the scope of applications of such materials in a variety of fields. Here, a facile and substrate-independent strategy for surface functionalization and patterning is presented. This approach combines the advantages of three important methods: facile and substrate-independent polydopamine coating, versatile gas phase silanization, and rapid thiol-ene photoclick reaction for patterning. They demonstrate equally efficient functionalization and patterning of diverse materials, such as glass, polytetrafluoroethylene, aluminum, polypropylene, or polyethylene. They also show the possibility of controlled chemical removal of the patterns or surface functionalization by treatment with tetrabutylammonium fluoride, which allows re-modification or re-patterning of the substrate. Thus, this universal and powerful approach for substrate independent surface modification and patterning can significantly facilitate the development of novel functional materials and devices useful for various applications.

1. Introduction

Surface functionalization through polydopamine (PDA) coating was introduced by Lee and Messersmith in 2007 and is a unique method inspired by the adhesive properties of the mussel foot.[1] The advantages of this technique include its simplicity, substrate-independence, robustness, and universality.[2–5] This substrate-independent coating method has been widely used in various applications, including surface patterning,[6–8] improving the biocompatibility of substrates,[9–11] and rendering surfaces superhydrophobic[12,13] or antibacterial.[14,15] The possibility of secondary modification, patterning, or the ability to re-functionalize PDA coatings is important to broaden the scope of applications of this coating method.[16,17] Various methods for the secondary modification of PDA coating, utilizing the presence of activated double-bonds, multiple catechol groups, and amino functionality in the PDA, have been introduced, including the use of thiols, amines, silanes, or various metal ions.[18–23]

The controllable aspects of the PDA coating secondary modification, including temporal and spatial control, are not as developed as the coating methods themselves. However, both spatial and temporal control play an important role in the subsequent application of such materials. In recent years, some researchers have proposed new solutions to accelerate the secondary modification of PDA coatings. Gu et al. accelerated the reductive deposition and oxidative removal of metal ions on a polydopamine

S. Li, J. M. Scheiger, Z. Wang, Z. Dong, P. A. Levkin
Institute of Biological and Chemical Systems-Functional
Molecular Systems (IBCS-FMS)
Karlsruhe Institute of Technology (KIT)
Hermann-von-Helmholtz-Platz 1
76344 Eggenstein-Leopoldshafen, Germany
E-mail: levkin@kit.edu

The ORCID identification number(s) for the author(s) of this article can be found under https://doi.org/10.1002/adfm.202107716.

A. Welle
Institute of Functional Interfaces (IFG) and Karlsruhe Nano
Micro Facility (KNMF)
Karlsruhe Institute of Technology (KIT)
Hermann-von-Helmholtz-Platz 1
76344 Eggenstein-Leopoldshafen, Germany

V. Trouillet
Institute for Applied Materials (IAM) and Karlsruhe Nano
Micro Facility (KNMF)
Karlsruhe Institute of Technology (KIT)
Hermann-von-Helmholtz-Platz 1
76344 Eggenstein-Leopoldshafen, Germany

P. A. Levkin
Institute of Organic Chemistry (IOC)
Karlsruhe Institute of Technology (KIT)
Kaiserstraße 12, 76131 Karlsruhe, Germany

**ADVANCED
SCIENCE NEWS**
www.advancedsciencenews.com

**ADVANCED
FUNCTIONAL
MATERIALS**
www.afm-journal.de

coating by ultraviolet irradiation to control the deposition of metal nanoparticles both spatially and temporally.[24] Several approaches for the patterning of PDA coatings have also been reported. Wu et al. demonstrated patterning of hydrophobic surfaces by negative microcontact printing of PDA.[6] Du et al. achieved patterning of PDA coatings on different materials through UV-triggered dopamine polymerization.[8] Behboodi-Sadabad et al. succeeded in the patterning of different phenolic compounds, which have similarities with dopamine.[25] In addition, Gu et al. achieved UV-assisted reversible deposition of metal ions on PDA coatings.[24] However, a reversible covalent modification of PDA coatings, which can greatly improve their reusability, has not been reported yet.

Here, we report a rapid and reversible strategy for the secondary modification and patterning of PDA coatings. This method is based on the secondary modification of PDA coatings by chlorosilanes, which allows fine-tuning of the surface energy and renders the surface patternable via the thiol-ene photoclick reaction. In addition, we demonstrate the feasibility of selectively removing the siloxane layer from the PDA modified surface using tetrabutylammonium fluoride (TBAF) solution. We provide a complete characterization of the method through contact angle (CA) measurement, atomic force microscopy (AFM), X-ray photoelectron spectroscopy (XPS), and time-of-flight secondary ion mass spectrometry (ToF-SIMS) analyses. Finally, we demonstrate the feasibility of functionalization and patterning of complex large-scale objects, which facilitates the practical application of the method. Thus, this strategy is an effective method for substrate-independent functionalization and patterning of a variety of surfaces.

2. Results and Discussion

The PDA coating was applied using the dipping method according to a previously reported oxidation deposition process.[1] In this step, we selected polytetrafluoroethylene (PTFE), polypropylene (PP), polyethylene (PE), aluminum (Al), and glass as substrates since these are commonly used industrially relevant materials (**Figure 1A**). All substrates appeared brown or light brown after modification with PDA (Figure 1B; Figure S1, Supporting Information). Evaluation of the surface morphology of the coating on a silicon wafer by AFM showed an increase in surface roughness after modification with PDA, with an increased R_q value from 0.14 ± 0.01 nm to 0.90 ± 0.04 nm (Figure 1C). The thickness of the PDA coating on the silicon wafer was measured as 14.1 ± 0.4 nm using the scratch method. In all cases, the static water contact angle (WCA) after the modification with PDA was similar and varied from 40° to 50° (Figure 1D). The XPS characterization also confirmed the successful functionalization (Figure 1E). In the PTFE/PDA sample, the C 1s peak from C—N for the PDA coating on PTFE was detected at 286.4 eV, while the C 1s peak from CF_2 at 292.4 eV was dramatically attenuated.

After applying the PDA coating, we used trichlorovinylsilane (TVS) to secondarily modify PDA coated substrates. The chlorosilane reacts with the amino and hydroxyl groups of the PDA coatings. Moisture from the surface and air further hydrolyzes the chlorosilane functionalities into silanol functional groups,

which condensate to a polysiloxane network and increase the thickness of the coating to 42.3 ± 2.9 nm. The silanization resulted in an increase in the WCA on PTFE, PP, PE, Al, and glass surfaces from $48 \pm 2°$, $47 \pm 2°$, $46 \pm 2°$, $46 \pm 2°$, and $41 \pm 2°$, respectively, to $84 \pm 1°$, $80 \pm 2°$, $82 \pm 1°$, $84 \pm 1°$, and $83 \pm 1°$, respectively (Figure 1D), demonstrating successful surface modification independent of the substrate used. In the XPS characterization, the Si $2p_{3/2}$ peak at 102.8 eV in the PTFE/PDA/TVS (the material names are given as "Substrate material/ first coating/secondary modification") sample also confirmed successful silanization (Figure S2, Supporting Information). The R_q value of the PDA/TVS-modified silicon wafer increased to 3.69 ± 0.43 nm, showing that TVS forms aggregates on the surface of the PDA (Figure 1C). The thickness of the PDA/TVS layer on the silicon wafer was 42.3 ± 2.9 nm, which was almost three times that of the PDA coating. In addition, we used trichloro($1H$,$1H$,$2H$,$2H$-perfluorooctyl)silane and trichloroethylsilane to test the reactivity of other chlorosilanes with PDA coatings. As shown in Figure S3, Supporting Information, the static WCA increased from 45° to 80° and 90°, respectively, after the silanization. In the case of trichloro($1H$,$1H$,$2H$,$2H$-perfluorooctyl)silane, the WCA was not as high as expected probably because its low vapor pressure reducing the density of functional groups after deposition.[26]

Substrates modified with TVS were then functionalized using the photoclick thiol-ene reaction. Different materials were covered with a $1H$,$1H$,$2H$,$2H$-perfluorodecanethiol (PFDT) solution and irradiated with 265 nm UV light (3.0 mW cm^{-2}) for 1 min through a quartz slide. The static WCA on PTFE, PP, PE, Al, and glass surfaces changed from $84 \pm 1°$, $80 \pm 2°$, $82 \pm 1°$, $84 \pm 1°$, and $83 \pm 1°$, respectively, to $124 \pm 1°$, $121 \pm 1°$, $119 \pm 2°$, $116 \pm 4°$, and $100 \pm 4°$, respectively (Figure 1D), thus confirming the success of the photoclick thiol-ene reaction. Compared with the PTFE/PDA/TVS sample, additional peaks (C 1s peak from CF_3 at 294.2 eV and C 1s peak from CF_2 at 292.0 eV) stemming from PFDT appeared in the XP spectra of the PTFE/PDA/F sample, confirming the successful modification with PFDT (Figure 1E). The corresponding F 1s peak at 689.1 eV, typical of a covalently bound fluorine, was also observed (Figure S4, Supporting Information). To demonstrate universality of the photoclick thiol-ene reaction on the PDA/ TVS coating, we functionalized the vinyl-bearing surfaces with hydrophilic thiol 2-mercaptoethanol (ME) in the same way. The static WCA on PTFE, PP, PE, Al, and glass surfaces changed from $84 \pm 1°$, $80 \pm 2°$, $82 \pm 1°$, $84 \pm 1°$, and $83 \pm 1°$, respectively, to $43 \pm 3°$, $45 \pm 2°$, $44 \pm 1°$, $56 \pm 2°$, and $44 \pm 3°$, respectively, indicating successful completion of the reaction and substrate independency (Figure 1D). At the same time, the S $2p_{3/2}$ peak at 163.9 eV appeared in both the PTFE/PDA/F and PTFE/ PDA/OH samples, indicating that both PFDT and 2-mercaptoethanol (ME) had clicked to the siloxane surface successfully (Figure 1F). PDA coatings can also react with thiols,[1] here, we reacted PFDT and ME with PDA coatings directly and characterized them by XPS as a comparison of our method. As shown in Figure S5, Supporting Information, the fluorine content measured by XPS increased from 5.7 atomic percentage (at%) to 12.9 at% after reacting PFDT directly with the PDA layer. However, the difference was much less marked than that achieved with the thiol-ene reaction (from PDA/TVS 0.9 at%
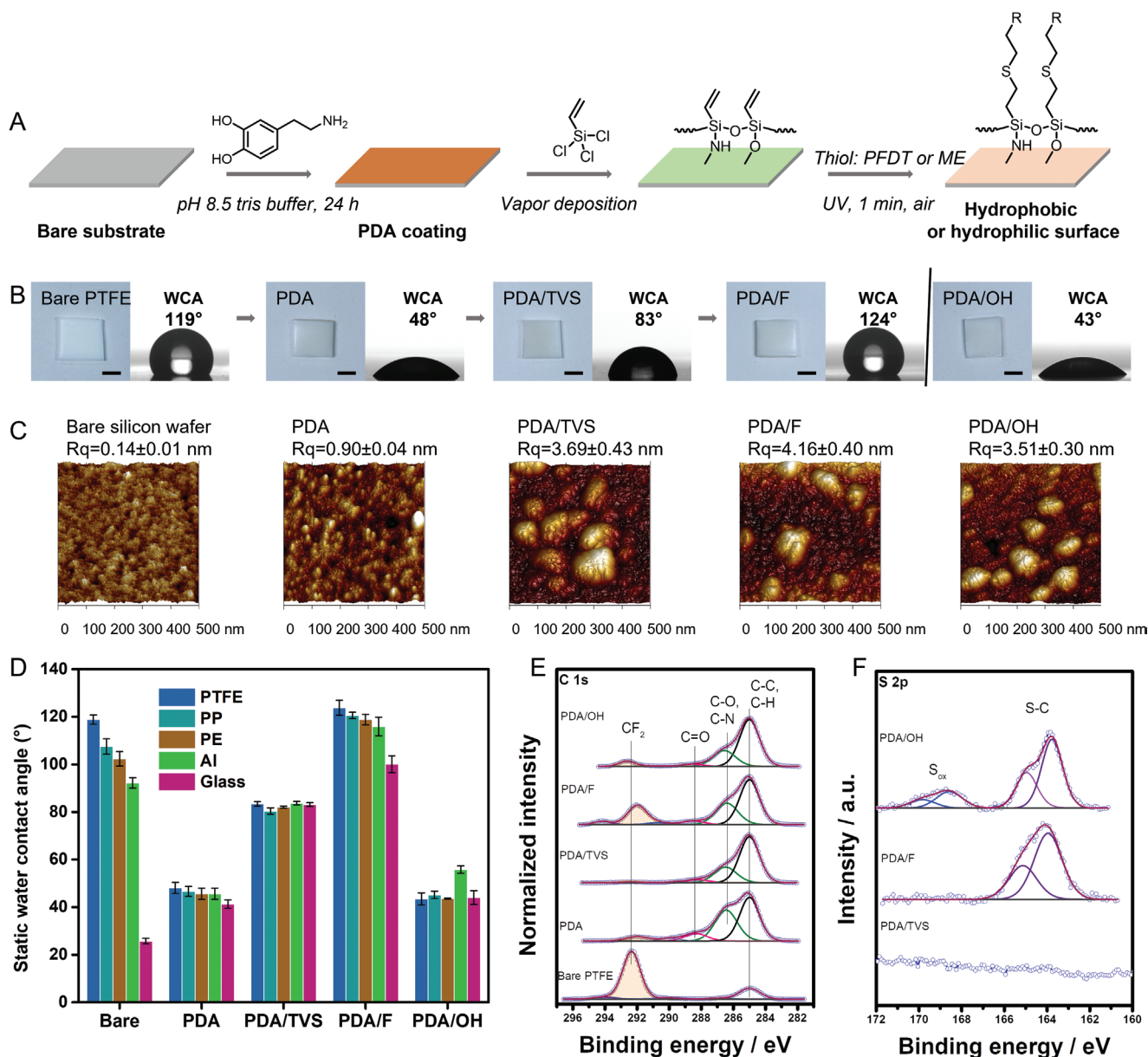
Figure 1. Substrate-independent surface functionalization by combining polydopamine coating, silanization by TVS (trichlorovinylsilane) and UV-induced thiol-ene reaction. A) Schematic representation of the PDA deposition, TVS silanization, and UV-induced thiol-ene photoclick processes. B) Digital images of modified PTFE slides and 2-μL water droplets on modified PTFE slides. Scale bar: 5 mm. C) AFM 3D images of different modified silicon wafers. D) Static WCA of bare substrates and surfaces with PDA coatings, followed by silanization (PDA/TVS), and thiol grafting (PDA/F and PDA/OH, respectively). E) C 1s XP spectra of different PTFE modification steps. F) S 2p XP spectra of PDA/TVS, PDA/F, and PDA/OH modified PTFE. Bare: bare substrates; PDA: PDA modified surface; PDA/TVS: PDA and TVS-modified surface; PDA/F: 1*H*,1*H*,2*H*,2*H*-perfluorodecanethiol (PFDT) click on PDA/TVS surface; PDA/OH: 2-mercaptoethanol (ME) click on PDA/TVS surface.

to PDA/TVS/F 27.1 at%). As a marker of the PDA layer, the nitrogen signal was also followed in parallel with these reaction steps. The nitrogen concentration did not decrease significantly after the reaction of PDA with either PFDT or ME, whereas a non-negligible decrease in the nitrogen fraction was observed after the thiol-ene click reaction (Figure S5, Supporting Information), indicating that the PDA-thiol reaction is much slower than the thiol-ene click reaction. In addition, the secondary modification of the PDA coating became reversible through the fluoride-induced desilylation (vide infra).

Chlorosilanes are commonly used as surface modification reagents; therefore, we compared direct modifications based on bare substrates using our PDA-based approach. We silanized bare substrates, performed photoclick thiol-ene reactions, and then measured the WCAs of the resulting surfaces (Figure S6, Supporting Information). While the glass sample showed a significant change as expected, the WCAs of the PTFE and Al samples hardly changed after both the TVS treatment and the photoclick thiol-ene reaction. TVS reacts with hydroxyl group on glass, thus TVS aggregates attach readily to the glass surface.[27]

Due to the absence or low density of OH groups on the surfaces of bare PTFE or Al, modification of these surfaces by TVS was not possible. For bare PP and PE, a small amount of TVS aggregates attached to the surface, causing small changes in the WCA and WCA hysteresis after the photoclick thiol-ene reaction with PFDT and ME (Figure 1D; Figure S6 and Table S1, Supporting Information). This showed that the PDA layer effectively changed the surface properties of the substrates, facilitating their subsequent modification. Thus, the introduction of PDA drastically improves the substrates compatibility with chlorosilanes.

The hydrolytic stability of the PDA/TVS layer and thiol click layers was investigated by monitoring the static WCA at different times after immersing the substrates in a 1:1 ethanol/water mixture for 72 h (Figure S7, Supporting Information). In the first 24 h, the static WCA of the PDA/TVS layer on all substrates decreased by several degrees. With the exception of glass, the static WCA of all substrates remained constant after immersion for more than 24 h (Figure S7A, Supporting Information). After 72 h, the static WCA of all substrates was higher than 70° and the large difference compared with the static WCA of PDA was retained (Table S2, Supporting Information). After click reaction with PFDT, all coatings were much more stable and the static WCA did not change significantly after 72 h. The hydrophilic thiol modified layer on PTFE, PE, and Al remained hydrophilic after 72 h (Figure S7B, Supporting Information). In addition to the broad applicability on several substrate materials, the stability of the PDA/TVS layer and the thiol-ene post-modifications is of great significance to their practical applications.

The advantage of our method is that PDA coating is substrate independent, thus allowing us to pattern various materials using essentially the same protocol. To demonstrate this universality, we reacted PDA/TVS-modified substrates with PFDT by UV irradiation for 1 min through a photomask (Figure S8, Supporting Information) to generate hydrophobic pattern. After washing with acetone and reaction with hydrophilic ME under UV for a further 1 min, the region of the surface that did not react with PFDT in the previous step was rendered hydrophilic (**Figure 2A**). ToF-SIMS imaging of OH⁻ and CF₃⁻ secondary ions showed the patterning of ME and PFDT on PP, PE, and PTFE coated with PDA (Figure 2C; Figure S9, Supporting Information). The pattern fidelities at the edge of the obtained 1-mm squares were below 100 μm (≈20 μm on PP and PE, and ≈80 μm on PTFE). These results showed that TVS modification of PDA coating can be used to achieve accurate spatial programing of the surface of various materials. Different types of hydrophilic–hydrophobic patterns were created on PTFE, PP, Al, and glass. Water flowed across the microscopic PFDT-ME-patterned surface of PP, with spontaneous dewetting of the PFDT areas to form an array of separated droplets located on ME-modified areas. A precise and continuous winding route
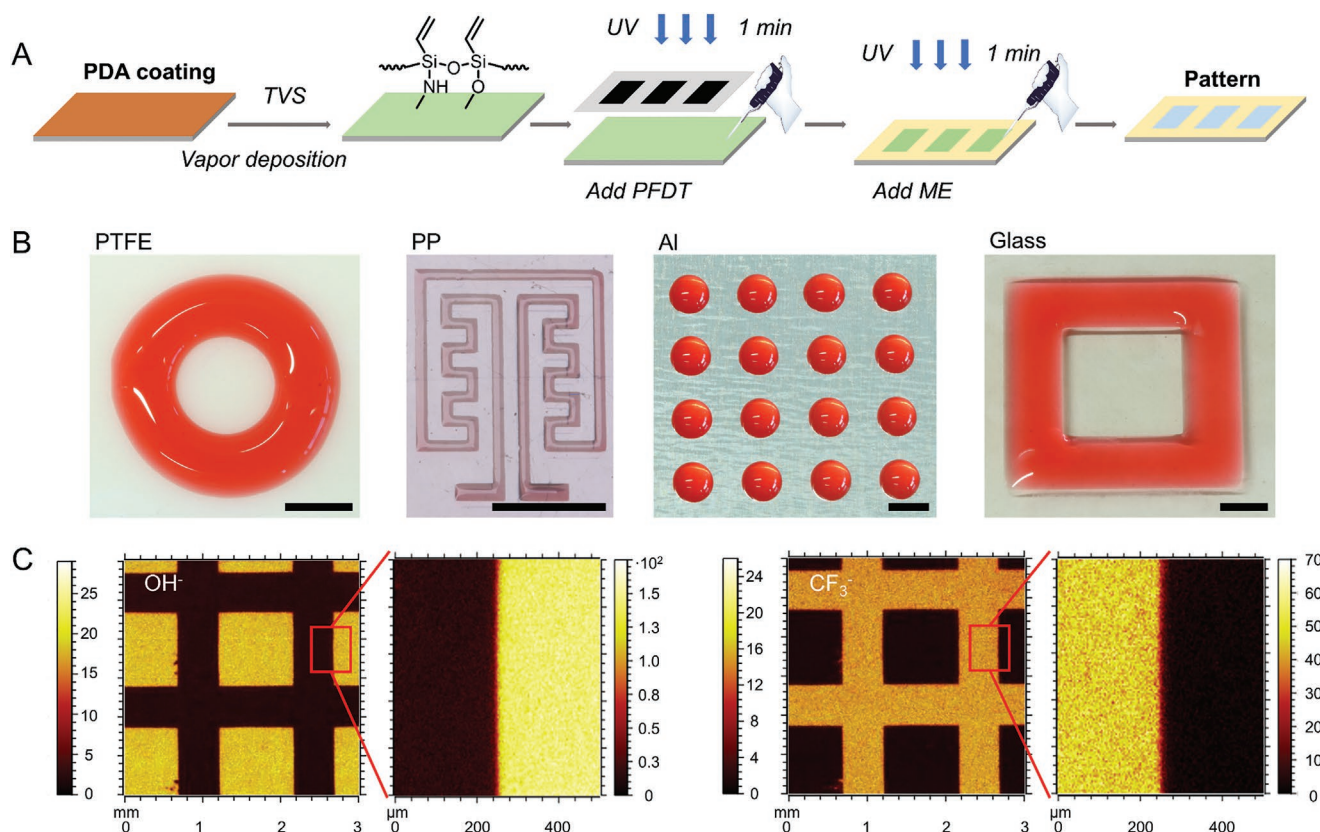

Figure 2. Substrate-independent patterning of TVS modified PDA-coated surfaces via UV-induced thiol-ene click reaction. A) Schematic representation of the silanization reaction and UV-induced thiol-ene photoclick reactions used to create hydrophilic–hydrophobic patterns on PDA coated substrates. B) Water pattern on hydrophilic–hydrophobic pattern produced on various substrates: PTFE, PP, Al, and glass. Water containing a food dye. Scale bar: 3 mm. C) ToF-SIMS 2D images of negative OH⁻ and CF₃⁻ secondary ions, showing the patterning of ME and PFDT on PP coated with PDA, respectively.
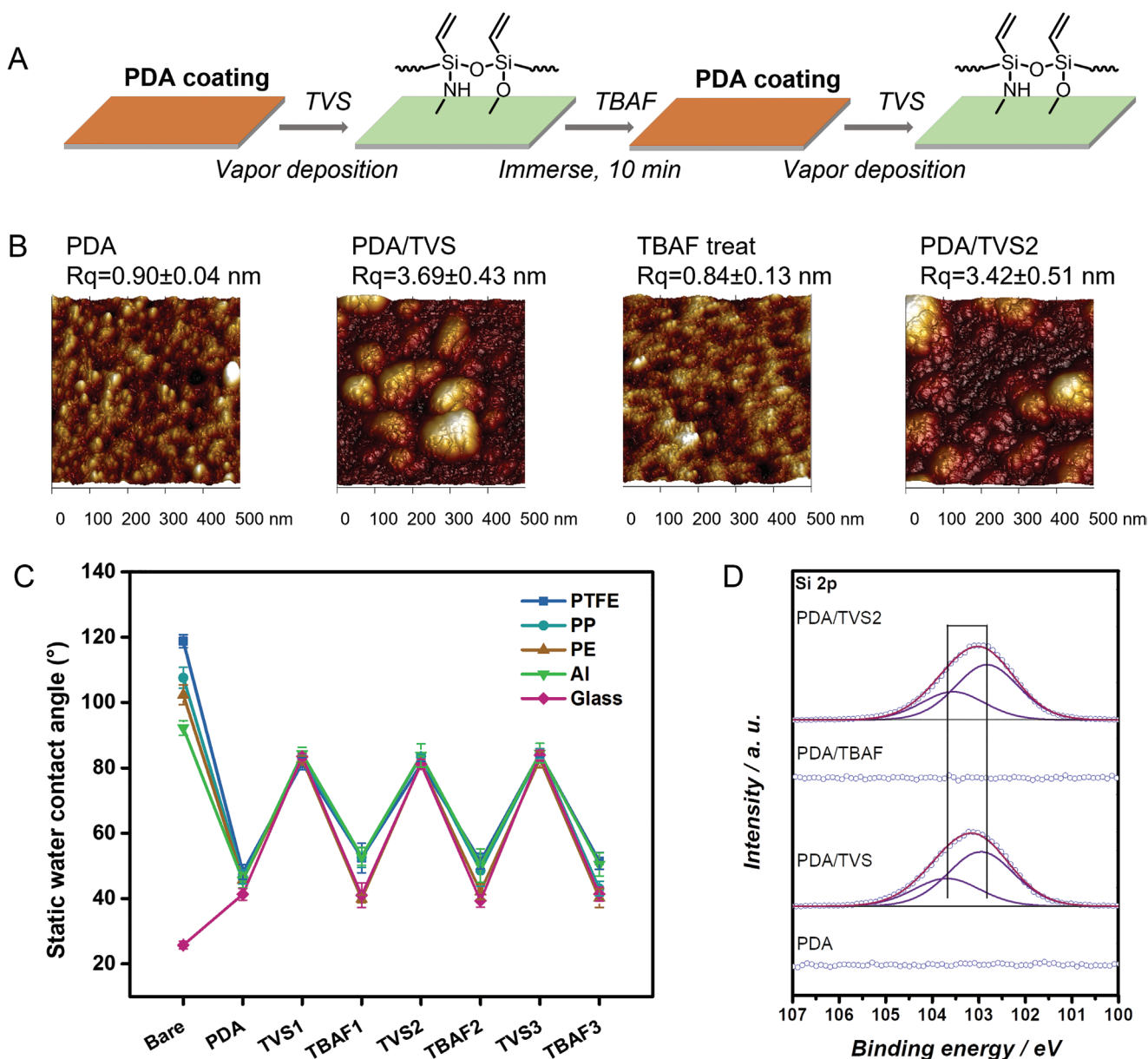
Figure 3. Reversible silanization process on PDA-coated substrates. A) Schematic representation of the process to reverse the TVS-modified PDA coating. B) AFM images of PDA, PDA/TVS, PDA/TBAF, and PDA/TVS2 modified silicon wafers. C) Static WCA changes of PDA-coated PTFE, PP, PE, Al, and glass treated with TVS and TBAF. D) Si 2p XP spectra of PDA, PDA/TVS, PDA/TBAF, and PDA/TVS2 modified PP. Bare: bare substrates; PDA: PDA modified surface; PDA/TVS: PDA and TVS-modified surface; PDA/TBAF: TBAF treated PDA/TVS surface; PDA/TVS2: TVS silanization on PDA/TBAF.

pattern with a path width of 350 μm was obtained on PP. For large-scale patterns on PTFE, Al and glass, water was added by pipetting to form a pattern on the hydrophilic area (Figure 2B).

Recently, we demonstrated the use of silanization and desilanization for creating, erasing, and re-writing the surface wettability patterns on polymer and silicon substrates. Reversible and versatile control of surface wettability was achieved by modifying the hydrophilic surface with fluorinated alkyl silane, followed by removing the functionalization by fluoride anions.[28] This dynamic and reversible process is of great significance for the recovery and reuse of substrates. To demonstrate the desilanization process on PDA coatings, TVS

silanized PDA pre-coated substrates were treated with TBAF solution for 10 min. AFM images showed that the surface became smoother after TBAF treatment, with a similar R_q value 0.84 ± 0.13 nm to that of the unmodified PDA coating on silicon wafers (0.90 ± 0.04 nm, **Figure 3B**). The static WCA of surfaces treated with TBAF on different substrates ranged from 40° to 50°, which is almost the same as that of the original PDA coating (Figure 3C). After re-silanizaton of the TBAF treated surfaces with TVS, the static WCA was restored to 80°. Repeatability of the process was demonstrated by multiple cycles of desilanization and silanization (Figure 3C). After three cycles, the original hydrophilicity of PTFE, PP, PE, Al,
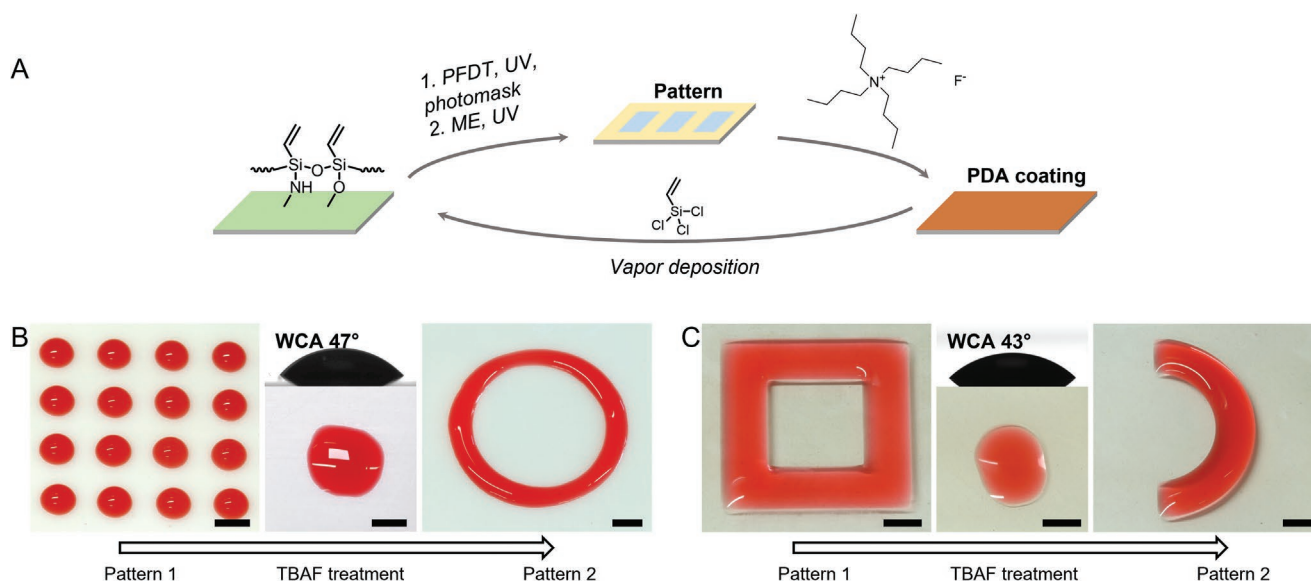
Figure 4. Writing, erasing, and re-writing patterns on PDA-coated materials using TBAF treatment. A) Schematic representation of the process to erase and re-write patterns on PDA coating using the TBAF treatment. B) Examples of the possibility to reversibly create functional chemical patterns on PTFE substrates with PDA coating. Left: round hydrophilic spots (patterned with ME) show the water droplet array on PTFE (pattern 1); middle: pattern 1 erased by TBAF treatment; right: new pattern prepared on PDA coated PTFE substrates. C) Pattern reversibility on PDA coated glass substrates. Left: hydrophilic square on glass filled with water (pattern 1); middle: pattern 1 erased by TBAF treatment; right: new pattern prepared on the TBAF treated area. Scale bar: 3 mm.

and glass with PDA coating was maintained, with static WCA ranging from 40° to 50° (Figure 3C). Silanization and desilanization was correlated with the presence and absence of the Si 2p doublet (with Si $2p_{3/2}$ at 102.8 eV), respectively (Figure 3D). Finally, we demonstrated that the reversible process was successful after the TVS layer was reacted with thiols. After PFDT was clicked under UV, the static WCA on different substrates increased to more than 100°. After treatment with TBAF solution in the same way as the TVS-modified substrates, the hydrophilicity of the surfaces was restored and the static WCA dropped to 40° (Figure S10, Supporting Information). This reversible process was shown to be repeated successfully in multiple cycles. Thus, combining PDA coating and silanization allows rapid and accurate definition of the properties of a variety of substrates. Furthermore, repeated patterning of surfaces can be achieved by TBAF desilanization to restore hydrophilicity of the original PDA coating. Following this process, a new pattern can be generated on the same substrate by silanization and the UV-induced thiol-ene click reaction (**Figure 4A**). As shown in Figure 4B, the hydrophilic pattern filled with water was created on PTFE and the entire surface was rendered hydrophilic by TBAF treatment. The surface was then silanized and clicked with PFDT and ME to create a new circular water pattern on the PTFE. The square pattern was also removed and a new semicircle pattern created on glass with PDA coating (Figure 4C).

PDA-based surface coating method offers the advantage of substrate-independency and simplicity. In addition, the dip-coating method allows modification of large objects with complex shapes in a single step process. As our patterning method is based on the use of PDA coating as the first layer, the method benefits from these same advantages. To demonstrate

the feasibility of functionalization and patterning of complex large-scale objects, we performed modification and patterning on various objects (soft adhesive PE tape, a plant leaf, a plastic flabellum, and a metal spoon). After PDA coating, TVS modification, and patterning (hydrophobic PFDT and hydrophilic ME reacted by thiol-ene click reaction), hydrophilic–hydrophobic patterns formed on the objects and could be visualized by water patterns confined by the hydrophobic regions (**Figure 5**; Figure S11, Supporting Information). Thus, the method allows us to create chemical patterns on flexible, natural, curved, and large substrates in only three steps.

3. Conclusions

In summary, we have established a rapid, facile, and substrate-independent strategy for reversible surface modification and patterning. This strategy is based on three steps: polydopamine coating, functionalization of polydopamine using trichlorovinyl-silane, and UV-induced modification or patterning using thiol-ene reaction. We have demonstrated that this method can be extended to a variety of substrates, including polytetrafluoroethylene, polypropylene, polyethylene, aluminum, and glass, using essentially the same procedure for all substrates. We further investigated reversibility of the silanization step and re-usability of patterned substrates to create new patterns on the same surface in multiple cycles of silanization and desilanization. This is important for the reuse of surfaces and for achieving higher flexibility in applications of PDA-coated surfaces. Finally, we demonstrated that the versatility of polydopamine coatings allows for the modification and patterning of complex large-scale objects, such as soft adhesive polyethylene tape, plant
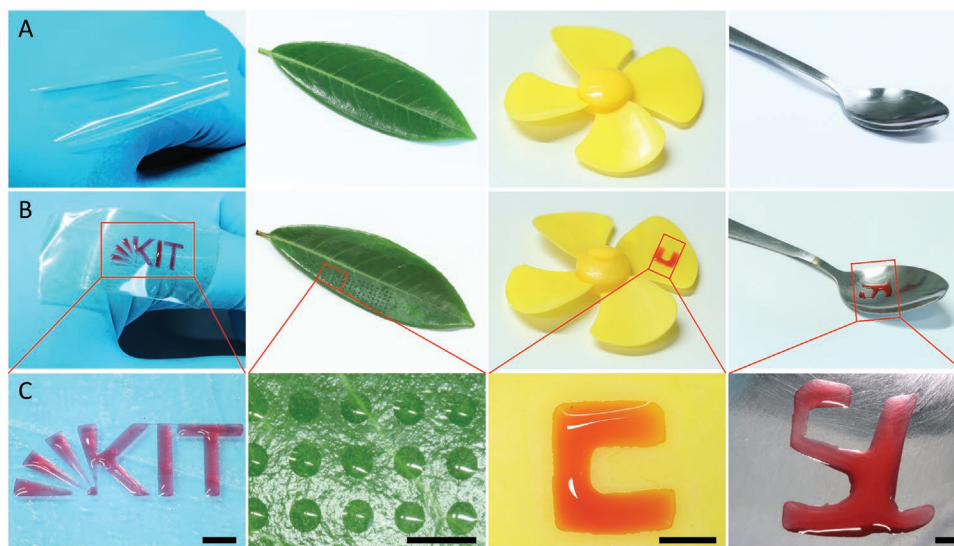
Figure 5. Application of the PDA/TVS modification strategy on complex-shaped large objects: soft adhesive PE tape, a plant leaf, a plastic flabellum, and a metal spoon. Digital images of objects before (A) and after (B) modification. C) Water pattern on objects (red patterns contain food dye). From left to right: Pattern on soft adhesive PE tape; array of round hydrophilic spots on a fluorinated plant leaf; letter "C" on a plastic flabellum; letter "SL" on a metal spoon. Scale bar: 3 mm.

leaves, plastic flabellum, and metal objects. Thus, our universal and simple approach for substrate independent surface modification and patterning will help in the development of novel functional materials, surfaces, and devices, which can be useful in myriads of applications.

4. Experimental Section

Chemicals and Materials: 3-Hydroxytyramine hydrochloride (99%) and tetrabutylammonium fluoride hydrate (99%) were purchased from Acros Organics (Geel, Belgium). Isopropanol, ethanol, and acetone were obtained from Merck (Darmstadt, Germany). All other chemicals were purchased from Sigma-Aldrich (Darmstadt, Germany) and used without further purification. PTFE plates, PP plates, PE adhesive tape, and aluminum adhesive tape were purchased from RS Components GmbH (Frankfurt, Germany) and were cut to the desired size for use. NEXTERION B glass slides were obtained from Schott AG (Mainz, Germany) and silicon wafers (CZ-Si-wafer 50 mm) were obtained from Siegert Wafer (Aachen, Germany). Tris buffers were prepared at a 10 mM and adjusted to pH 8.5 using a Mettler Toledo digital pH meter (Shanghai, China).

Preparation of PDA Coatings: PTFE, PP, PE, and Al slides were cut to the desired size (usually 2.1 cm × 7.6 cm). Glass slides were used as purchased (2.1 cm × 7.6 cm). All slides were washed with isopropanol, ethanol, and deionized (DI)-water, then immersed in 2 mg mL^{-1} 3-hydroxytyramine hydrochloride tris solution (tris solution: 10 mM, pH 8.5) for 24 h. The slides were then rinsing thoroughly with DI water and dried.

Vapor Deposition: PDA-coated substrates were placed in a desiccator containing an open vial with 0.5 mL trichlorovinylsilane (TVS). The desiccator was evacuated and left closed for 15 min. The reaction was performed in the gaseous phase at room temperature. Leave the samples in a fume hood for half an hour until the hydrochloric acid produced in the reaction has evaporated. All samples were then washed with ethanol and DI water and dried.

UV-Induced Thiol-Ene Photoclick: For fully reacted samples, TVS-modified substrates were wetted with acetone solution of 10 vol% of PFDT or ME, and irradiated with 3.0 mW cm^{-2} 265 nm UV light for

1 min. The samples were then washed several times with acetone and dried with airflow.

For patterning samples, substrates were wetted with a 10 vol% solution of PFDT in acetone, covered by a quartz photomask, and irradiated with an intensity of 3.0 mW cm^{-2} and a wavelength of 265 nm (UV) light for 1 min. The distance between substrates and photomasks were controlled by placing 200 μm polyimide spacers between them. Samples were then washed several times with acetone and dried with airflow. Next, substrates were wetted with a 10 vol% solution of ME in acetone and irradiated with an intensity of 3.0 mW cm^{-2} and a wavelength of 265 nm (UV) light for 1 min. The samples were washed several times with acetone and dried with airflow.

Degradation of Siloxane Layer with TBAF: TVS silanized substrates with PDA coating were immersed into 0.1 M TBAF ethanol solution. After a 10 min treatment, the substrates were washed with ethanol and deionized water then dried.

CA Measurement: The static WCA (≈2 μL) on bare and modified substrates was measured using a DSA25S drop shape analyzer (Krüss, Hamburg, Germany). Advancing WCA values were obtained by measuring the WCA while the liquid was slowly added (at 0.2 μL s^{-1}) to increase the volume of droplet from ≈5 to ≈15 μL in contact with the sample using a micrometer syringe. Receding WCA values were obtained by slowly retracting the liquid (0.2 μL s^{-1}) to decrease the volume of the droplet from a 15 μL droplet to 5 μL.

Atomic Force Microscopy: AFM was performed on a Dimension Icon AFM (Bruker, Karlsruhe, Germany) in standard tapping mode under air (INT, KIT). Cantilevers (HQ/NSC15/Al BS; MikroMasch) were used with a nominal force constant of 40 N m^{-1} and a resonance frequency of 325 kHz.

Time-of-Flight Secondary Ion Mass Spectrometry: ToF-SIMS analysis was performed using a TOF-SIMS.5 spectrometer (IONTOF GmbH, Münster, Germany) at IFG, KIT. A bunched primary beam of 25 keV Bi$_3^+$ ions was applied (10 kHz, 0.33 pA target current, ≈1 ns pulse width). Mass scale calibration was based on C$^-$, CH$^-$, CF$^-$, C$_2^-$, and C$_3^-$ signals. Large field of view images were obtained by rastering the primary ion beam and the sample stage, whereas 500 × 500 μm^2 images were obtained by rastering the primary beam alone (dose density 2 × 10^{11} ions cm^{-2}, 128 × 128 pixels). Charge compensation was achieved using an electron flood gun (21 eV) and time-of-flight analyzer tuning. Intensity traces were obtained by summing the signals of given secondary ions (devoid of detector saturation) from pixels parallel to the pattern border (image

de-rotating and summing) and calculating the spacing between 16% and 84% of the total signal step.

X-Ray Photoelectron Spectroscopy: XPS analysis was performed using a K-Alpha+ XPS spectrometer (Thermo Fisher Scientific, East Grinstead, UK), IAM, KIT. Thermo Avantage software was used for data acquisition and processing. All surfaces were analyzed using a microfocused, monochromated Al Kα X-ray source (400 µm spot size). The K-Alpha+ charge compensation system was employed during analysis, using electrons of 8 eV energy, and low-energy argon ions to prevent any localized charge build-up. The spectra were fitted with one or more Voigt profiles (BE uncertainty: ±0.2 eV) and Scofield sensitivity factors were applied for quantification.[29] All spectra were referenced to the C 1s peak (C—C, C—H) at 285.0 eV binding energy controlled by means of the well-known photoelectron peaks of metallic Cu, Ag, and Au.

Digital Photography: Digital photos were taken using a Canon EOS 80D digital camera.

Supporting Information

Supporting Information is available from the Wiley Online Library or from the author.

Conflict of Interest

The authors declare no conflict of interest.

Data Availability Statement

The data that support the findings of this study are available from the corresponding author upon reasonable request.

[1] H. Lee, S. M. Dellatore, W. M. Miller, P. B. Messersmith, *Science* **2007**, *318*, 426.
[2] J. H. Ryu, P. B. Messersmith, H. Lee, *ACS Appl. Mater. Interfaces* **2018**, *10*, 7523.
[3] H. Yang, R. Z. Waldman, M. Wu, J. Hou, L. Chen, S. B. Darling, Z. Xu, *Adv. Funct. Mater.* **2018**, *28*, 1705327.
[4] S. H. Hong, S. Hong, M. Ryou, J. W. Choi, S. M. Kang, H. Lee, *Adv. Mater. Interfaces* **2016**, *3*, 1500857.
[5] M. Ryou, Y. M. Lee, J. Park, J. W. Choi, *Adv. Mater.* **2011**, *23*, 3066.
[6] H. Wu, L. Wu, X. Zhou, B. Liu, B. Zheng, *Small* **2018**, *14*, 1802128.
[7] X. Du, L. Li, F. Behboodi-Sadabad, A. Welle, J. Li, S. Heissler, H. Zhang, N. Plumeré, P. A. Levkin, *Polym. Chem.* **2017**, *8*, 2145.
[8] X. Du, L. Li, J. Li, C. Yang, N. Frenkel, A. Welle, S. Heissler, A. Nefedov, M. Grunze, P. A. Levkin, *Adv. Mater.* **2014**, *26*, 8029.
[9] S. H. Ku, J. Ryu, S. K. Hong, H. Lee, C. B. Park, *Biomaterials* **2010**, *31*, 2535.
[10] X. Zhou, H. Cui, M. Nowicki, S. Miao, S. Lee, F. Masood, B. T. Harris, L. G. Zhang, *ACS Appl. Mater. Interfaces* **2018**, *10*, 8993.
[11] H. Cui, W. Wang, L. Shi, W. Song, S. Wang, *Small Methods* **2020**, *4*, 2000573.
[12] C. Chang, K. W. Kolewe, Y. Li, I. Kosif, B. D. Freeman, K. R. Carter, J. D. Schiffman, T. Emrick, *Adv. Mater. Interfaces* **2016**, *3*, 1500521.
[13] L. Zhang, J. Wu, Y. Wang, Y. Long, N. Zhao, J. Xu, *J. Am. Chem. Soc.* **2012**, *134*, 9879.
[14] J. Zhu, A. Uliana, J. Wang, S. Yuan, J. Li, M. Tian, K. Simoens, A. Volodin, J. Lin, K. Bernaerts, Y. Zhang, B. Van der Bruggen, *J. Mater. Chem. A* **2016**, *4*, 13211.
[15] W. Lei, K. Ren, T. Chen, X. Chen, B. Li, H. Chang, J. Ji, *Adv. Mater. Interfaces* **2016**, *3*, 1600767.
[16] X. Wan, X. Xu, X. Liu, L. Jia, X. He, S. Wang, *Adv. Mater.* **2021**, *33*, 2008557.
[17] F. Zhang, J.-b. Fan, S. Wang, *Angew. Chem., Int. Ed.* **2020**, *59*, 21840.
[18] H. A. Lee, E. Park, H. Lee, *Adv. Mater.* **2020**, *32*, 1907505.
[19] T. Tran, X. Chen, S. Doshi, C. M. Stafford, H. Lin, *Soft Matter* **2020**, *16*, 5044.
[20] D. Yang, M. Ruan, S. Huang, Y. Wu, S. Li, H. Wang, Y. Shang, B. Li, W. Guo, L. Zhang, *J. Mater. Chem. C* **2016**, *4*, 7724.
[21] X. Wan, Y. Zhan, Z. Long, G. Zeng, Y. Ren, Y. He, *Appl. Surf. Sci.* **2017**, *425*, 905.
[22] D. Yang, M. Ruan, S. Huang, Y. Wu, S. Li, H. Wang, X. Ao, Y. Liang, W. Guo, L. Zhang, *RSC Adv.* **2016**, *6*, 90172.
[23] Z. Liu, Y. Hu, C. Liu, Z. Zhou, *Chem. Commun.* **2016**, *52*, 12245.
[24] Y. Zeng, X. Du, W. Hou, X. Liu, C. Zhu, B. Gao, L. Sun, Q. Li, J. Liao, P. A. Levkin, Z. Gu, *Adv. Funct. Mater.* **2019**, *29*, 1901875.
[25] F. Behboodi-Sadabad, H. Zhang, V. Trouillet, A. Welle, N. Plumeré, P. A. Levkin, *Adv. Funct. Mater.* **2017**, *27*, 1700127.
[26] M. Psarski, G. Celichowski, E. Bystrzycka, D. Pawlak, J. Grobelny, M. Cichomski, *Mater. Chem. Phys.* **2018**, *204*, 305.
[27] A. Y. Fadeev, T. J. McCarthy, *Langmuir* **2000**, *16*, 7268.
[28] M. Brehm, J. M. Scheiger, A. Welle, P. A. Levkin, *Adv. Mater. Interfaces* **2020**, *7*, 1902134.
[29] J. H. Scofield, *J. Electron Spectrosc. Relat. Phenom.* **1976**, *8*, 129.